Reviewer #2

General comments:

This paper describes an improved droplet freezing instrument and gives examples of its performance. The authors took care to account and correct for temperature gradients within the plate by applying a rigorous temperature calibration. Like this, they achieve a temperature uncertainty of ± 0.6°C. Moreover, they developed user-friendly software with automatic freezing detection.

We would like to thank the reviewers for their thoughtful comments that helped improve our manuscript. We revised the manuscript accordingly and think it has strengthened as a result. Please find our point-by-point response in blue text. Additions to the text are shown in *italics with an underline*. All line numbers refer to the new version of the draft. A tracked changes version is also included.

To achieve the low temperature uncertainty of ± 0.6°C, the temperature of each individual well is measured with an infrared camera. These measurements show a temperature increase in two steps due to the heat release during freezing over a temperature decrease of the ethanol bath by about 1°C. The authors assign ice nucleation to the first heat release without explaining why. Yet, to achieve the high accuracy of ± 0.6°C, the correct detection of the instance of ice nucleation is crucial. If the exact instance of ice nucleation is not identified, this will add to the temperature uncertainty.

Thank you for your comment. We agree that detecting the instance of ice nucleation is critically important. This comment is related to your later specific comment in Lines 153–155 and Figure 3.

Figure 3 demonstrates a decrease in grayscale as the chamber cools. The figure should be interpreted from right to left, as the experiment represents a cooling process. Consequently, the first significant change in grayscale indicates the onset of ice nucleation. The second change in grayscale is caused by the freezing of the remaining droplet solution (David et al., 2019). We have also checked previously published papers, and most figures depict the temperature decrease from right to left. Therefore, we have decided to retain the figure as it is.

We modified the text accordingly: "*The grayscale value of a well stays constant until a sudden decrease is observed during a cooling experiment, indicating the onset of freezing. From 0.0 °C to −35.0 °C, the maximum decrease in grayscale value was used to identify the freezing event and the temperature at which it occurs.*"

Moreover, according to the infrared camera measured temperature during a cooling experiment (Fig. C1), only one latent heat release process happened. Similar to Fig. 5d in the manuscript, here we show the temperature profile of a well during the cooling process.

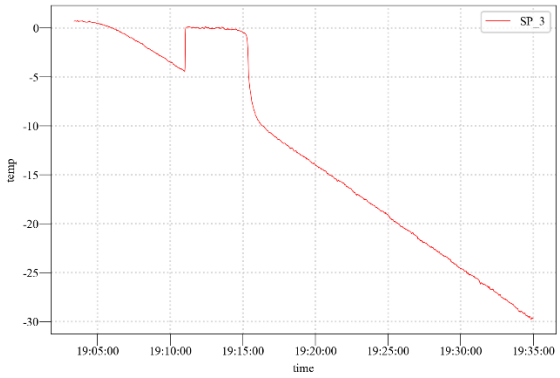

Fig. C1. The temperature profile of a well is measured by the infrared camera after its calibration.

To account for horizontal temperature differences within the well plate, a temperature correction for each well is performed. Such a correction requires that the wells' temperature deviations from the average of the thermocouples is highly reproducible. The authors need to evaluate this potential contribution to temperature uncertainty.

The horizontal temperature heterogeneity is caused by the ethanol circulation in the chiller, which has been discussed in previous studies, e.g., the DRoplet Ice Nuclei Counter Zurich (DRINCZ) (David et al., 2019), IR-NIPI (Harrison et al., 2018), and Micro-PINGUIN (Wieber et al., 2024). For a specific chiller and fixed temperature cooling rate, the temperature deviation is reproducible.

The horizontal temperature distribution might slightly change over time. To avoid a bias in the temperature calibration, we plan to conduct the whole temperature calibration procedure yearly.

Moreover, the freezing temperature measured for pure water should be compared to additional instruments.

Thanks for your suggestions. We compared with more DFT studies, including FINC (Miller et al., 2021), Micro-PINGUIN (Wieber et al., 2024), DRINCZ (David et al., 2019), IR-NIPI (Harrison et al., 2018), and INDA (Chen et al., 2018b).

Below is the updated Figure 8. Our Milli-Q water background (denoted by solid lines) is still one of the lowest among the above-mentioned studies. We changed the main text accordingly.

"The FF of Milli-Q water droplets using DFTs with different volumes, including Freezing Ice Nuclei Counter (FINC) (Miller et al., 2021), microtiter plate-based ice nucleation detection results in gallium (Micro-PINGUIN) (Wieber et al., 2024), Droplet Ice Nuclei Counter Zurich (DRINCZ) (David et al., 2019), InfraRed-Nucleation by Immersed Particles Instrument (IR-NIPI) (Harrison et al., 2018), and Ice Nucleation Droplet Array (INDA) (Chen et al., 2018b), are shown in Fig. 8 for comparison. In general, FINDA-WLU (T_{50} = –26.5 ± 0.04℃) shows a considerably lower T_{50} compared to those measured by INDA (T_{50} = –25.5 ℃), FINC (T_{50} = –25.4 ℃), DRINCZ (T_{50} = –22.2 ℃), IR-NIPI (T_{50} = –21.0 ℃), and Micro-PINGUIN (T_{50} = –20.8 ℃)."

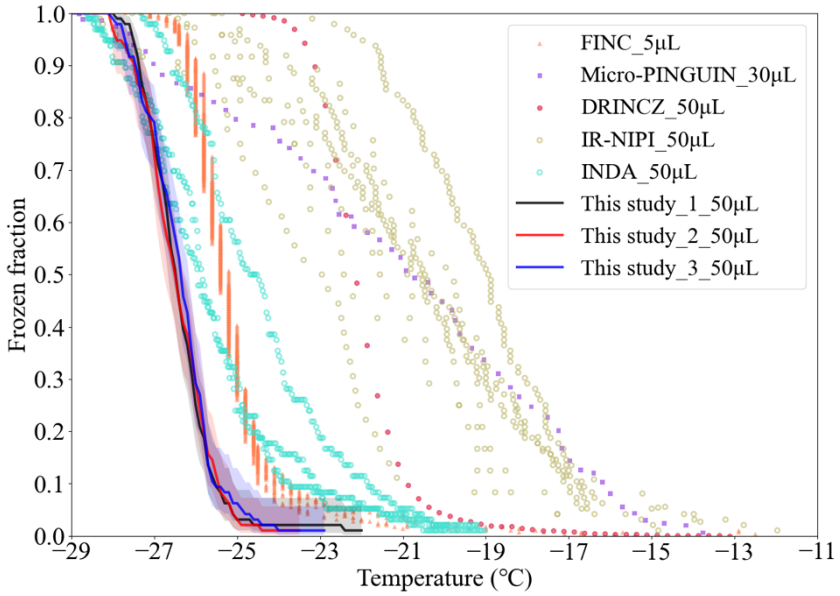

"*Figure 8: Frozen fraction of Milli-Q water. The results of FINDA-WLU are shown as solid lines. The shaded area indicate the measurement uncertainties. Results for other droplet freezing techniques, including FINC (Miller et al., 2021), Micro-PINGUIN (Wieber et al., 2024), DRINCZ (David et al., 2019), IR-NIPI (Harrison et al., 2018), and INDA (Chen et al., 2018b), are shown as triangles, squares, dots, and circles, respectively.*"

Overall, the manuscript is well written except for the introduction. Here, the strength and weaknesses of the different immersion freezing setups are not enough pointed out and discussed. The state of the art of freezing instruments does not discriminate sufficiently between different types of setups in terms of temperature range that is accessible and how the covered sample volume depends on the droplet preparation technique. Moreover, the references given in the introduction are not sufficiently balanced (see specific comments).

Thanks for your suggestion. As you mentioned, Miller et al. (2021) summarize different DFTs. Below, we have incorporated additional information—such as temperature cooling rate, temperature uncertainty, and T_{50} of water background—into a new table that is based on the original Table 1 from Miller et al. (2021). Nevertheless, given that Miller et al. (2021) have already presented the majority of the pertinent information, we have chosen not to include this table in the manuscript unless the reviewers strongly recommend otherwise.

We did modify the text in the introduction. A more detailed response is given in the specific comment.

Table 1. Comparison of droplet freezing techniques (DFTs).

Name	Description	Drop Size	Drops	T range (°C)	Cooling rate (K min-1)	T uncertainty (°C)	T_{50} of MilliQ (°C)	Citation

	combining microfluidic droplet generation and collection with a Peltier-based cold stage	83-99 μm; 2 μL add 2 μL oil	250-500	to −45 (Peltier)	1-10	0.5		Tarn et al., 2018
CMU-CS	the Carnegie Mellon University Cold Stage system	~ 0.1 μL	30-40	10 to −40	1	0.5		Polen et al., 2016
FDF	the combined membrane filter-drop freezing technique	1±0.1 μL	~ 40, maximum 130	to ~ −30	1	0.4 (μL-NIPI)	~ −27.5; ~ −30	Price et al., 2018; Schnell, 1982
μL-NIPI	the microlitre Nucleation by Immersed Particle Instrument	1±0.025 μL	~ 40	1 to −35	1	0.4	~ −26	Whale et al., 2015
BINARY	the Bielefeld Ice Nucleation ARraY	1 μL (0.5-5 μL)	36	5 to −40	1 (could be 0.1-10)	0.3		Budke and Koop, 2015
WACIFE	a Grant-Asymptote EF600 cold stage	1.0±0.1 μL, 60-129 μm	~ 33	to −40	1, 10	0.4	~ −26	Wilson et al., 2015
PKU-INA	PeKing University Ice Nucleation Array	1 μL	90	0 to −30	0.1-10	0.4	~ −28	Chen et al., 2018
LINA	Leipzig Ice Nucleation Array	1 μL	90	5 to −40 (same to BINARY)	1	0.5	~ −30	Chen et al., 2018
	a pyroelectric thermal sensor	1 μL		to −30	1	0.8		Cook et al., 2020
FRIDGE-TAU	FRankfurt Ice-nuclei Deposition freezinG Experiment, the Tel Aviv University version	2 μL	100-130	−18 to −27	1		−24	Ardon-Dryer et al., 2011
DFCP	the NOAA drop freezing cold plate	2.5 μL	100	to −33	1-10	0.2	~ −30	Baustian et al., 2010;
TINA	the Twin-plate Ice Nucleation Assay	3 μL (0.1-40 μL)	192, 768	−1.5 to −40.15	1-10	0.2	~ −26	Kunert et al., 2018
	a cold stage in single crystals	3 μL		10 to −30	3			Mignani et al., 2019
CRAFT	the Cryogenic Refrigerator Applied to Freezing Test	5 μL	49	50 to −80	1	0.2	~ −35	Tobo et al., 2016
FINC	Freezing Ice Nuclei Counter	5-60 μL	288	to −30	1	0.5	−25.2 (50μL)	Miller et al., 2021

	flow cell microscopy	20-22 µL		to −43.15, −93.15 (230 K, 180 K)	5	0.1		Koop et al., 2000
AIS	the Automated Ice Spectrometer	50 µL	192	15 to −33	0.69-0.87	horizontal 0.3; vertical 0.6		Beall et al., 2017
INSEKT	the Ice Nucleation SpEctrometer of the Karlsruhe Institute of Technology	50 µL	32 (192 in total)	0 to −25.15 (248 K to 268 K)	0.33	0.3		Schiebel, 2017(thesis)
IR-NIPI	the InfraRed-Nucleation by Immersed Particles Instrument	50 µL	96	to −90	1	0.9	~ −18 to −23	Harrison, et al., 2018
INDA	Ice Nucleation Droplet Array	50 µL	96	to −30	1	0.5	~ −14 to −16	Chen et al., 2018
DRINCZ	the DRoplet Ice Nuclei Counter Zurich	50 µL	96	0 to −30	1	0.9 (reproducible 0.3; horizontal 0.6)	~ −22.5	David et al., 2019
DFT	the droplet freezing technique	50 µL	48	0 to −30	0.67	1	~ −23	Gute and Abbatt, 2020
CSU-IS	CSU Ice Spectrometer	50 µL	32	to −30	0.33		start −25	Barry et al., 2021
	drop freezing apparatus for filters	0.1 mL	108	to −12	0.33 (record frozen per 1 °C)			Conen et al., 2012
	a high throughput screening platform involving microplates	150 µL	96-768	2 to −25	0.2			Zaragotas et al., 2016
LINDA	LED-based Ice Nucleation Detection Apparatus	200 µL (40-400 µL)	52	to −15	0.4	0.2 (repeated)		Stopelli et al., 2014
MINA	the mono ice nucleation assay		(PCR)	−5 to −15	2 for 12 min			Pummer et al., 2015
MOUDI −DFT	the micro-orifice uniform deposit impactor-droplet freezing technique (Chow and Watson, 2007)	0.056-18 µm		to −40	to −40	0.3		Mason et al., 2015
	droplet freezing technique	1-40 µm	200−800	−15.15 to −30.15	0.1			Dymarska et al., 2006

	flow cell microscopy technique for aerosol phase transitions	7-33µm	65	to −103.15	2−12	1 (0.1 at 0 °C)		Salcedo et al., 2000
Leeds−NIPI	Nucleation by Immersed Particle Instrument	10^{-12} to 10^{-6} L (8 µm to 1.45 mm)		−6 to −36	10	0.4		O'Sullivan et al., 2014
		10-40 µm	10−230	to −45.15 (228 K)	2.5−10	0.6	−32.35	Murray et al., 2010; Murray et al., 2011
		10-200 µm		~ 15.15 to −39.15	1−2	The Peltier element below 220K, <1	~ −36.15	Pummer et al., 2012
	a freezing chip	20-80 µm, 4-300 pL	~25	to −40	2	0.4	−37.5	Häusler et al.. 2018
	an FDCS196 cryostage	~ 35 µm	~200	to −40	1	0.1 (for TMS 94)	−9	Weng et al., 2017
WISDOM	The WeIzmann Supercooled Droplets Observation on Microarray	40, 100 µm	500, 120	13.15 to −38.15 (260 K to 235 K)	0.1−10	1		Reicher et al., 2018
	(Wright and Petters, 2013; Bigg, 1953)	50-300 µm	~100−500	−4 to −33	5	1		Wright et al., 2013
	the differential scanning calorimeter (DSC) measurements, and the cryo-microscope experiments	~53-96 µm	a few thousand	to −50	1 (from −10°C to lower temperature)	0.3		Riechers et al., 2013
	combining microfluidic droplet generation and collection with a Peltier−based cold stage	83-99 µm; 2 µL add 2 µL oil	250−500	to −45 (Peltier)	1−10	0.5		Tarn et al., 2018
SBM	soccer ball model (Niedermeier, 2011, 2014, 2015)	215±70 pL, 107±14 µm	1200−1500+	126.85 to −196.15	0.01−100	0.1 (from −40°C to 30°C)		Peckhaus et al., 2016
	a "store and create" microfluidic device	6 nL (5.8±0.7 nL) equal to 300±18 µm	720	0 to −33	1	0.2	−33.7±0.4	Brubaker et al., 2020

Specific comments:

In the title, the abstract, and in the text, the impression is given that the FINDA-WLU is based on a previous design that has been improved. Yet, no reference to the previous design is given. Please explain.

The first generation of FINDA was designed in 2021 by Kai Bi (one of our corresponding authors) from the Beijing Weather Modification Center. The original version FINDA was used to measure the INP of hailstones in China (details in Ren et al. (2024)). The new version was redesigned in cooperation with Westlake University. We updated the setup, hardware, and temperature calibration procedure for the version of FINDA-WLU.

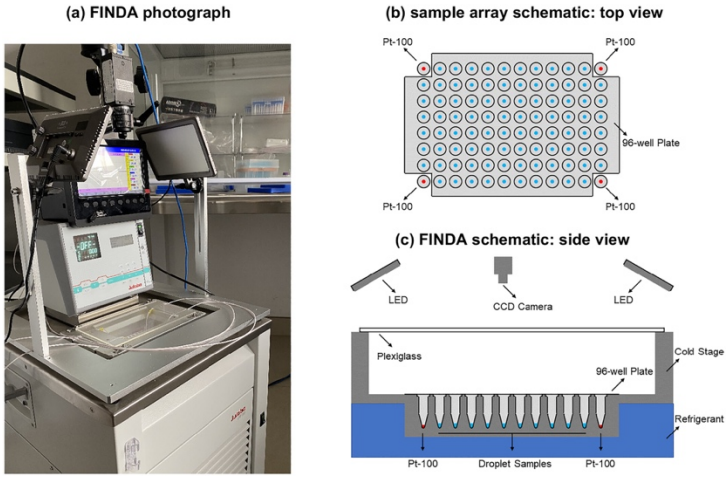

Fig. 2 in Ren et al. (2024) shows the original verion of FINDA.

Based on your suggestion, we modified the introduction to include this information. "*In this study, we present the newly developed Freezing Ice Nucleation Detector Array at Westlake University (FINDA-WLU), building on the original version of FINDA briefly introduced in Ren et al. (2024).*"

Lines 50–54: The references given for in-situ methods and laminar flow reactors are not sufficiently balanced and seem to have a bias to references from authors of the manuscript. Specific examples of ice nucleation chambers, laminar flow reactors, and droplet freezing devices should be given together with appropriate references. See Miller et al., 2021 for an overview of instruments.

Thanks for your suggestion.

Regarding the ice nucleation chambers and laminar flow reactors, we cited the CSU-CFDC (Rogers, 1988; Rogers et al., 2001; Demott et al., 2015), SPIN (Garimella et al., 2016), HINC (Lacher et al., 2017), PINC (Kanji et al., 2013), and PINE (Möhler et al., 2021a). Regarding the offline DFTs, we cited the CUS-IS (Hill et al., 2014), BINARY (Budke and Koop, 2015), FINC (Miller et al., 2021), PKU-INA (Chen et al., 2018a), INDA (Chen et al., 2018b), LINA (Chen et al., 2018b), IR-NIPI (Harrison et al., 2018), DRINCZ (David et al., 2019), and INSEKT (Steinke et al., 2020).

We modified the introduction accordingly, including the above-mentioned instrument papers.

Lines 61–64: "However, ice nucleation chambers and reactors are typically expensive and have higher detection limitations compared to DFTs, especially at higher temperatures (T > –20°C) where increased background noise caused by ice residues falling from chamber walls or counting statistics of low ice crystal numbers makes detecting INPs with low concentrations challenging." What is meant by "higher detection limitations"? To my knowledge, ice-nucleation chambers do not have a problem with falling ice. Please give references for this statement.

Thank you for pointing that out. Continuous Flow Diffusion Chambers (CFDCs) indeed suffer from the falling ice issue. We quote from Lacher et al. (2017), which explains the working principle of the Horizontal Ice Nucleation Chamber (HINC), a typical CFDC designed at ETH.

"*During an ice nucleation experiment, erroneous counts in the OPC ice channel can arise from electrical noise in the OPC or from internal ice sources such as frost falling off the warmer chamber wall giving rise to particle counts that are falsely classified as ice.*"

While an expansion chamber (e.g., PINE) does not encounter the falling ice issue, it can still produce erroneous counts in the OPC at warmer temperatures, especially when INP concentrations in the air are low. And generally, the optical detection of single frozen droplets as used in ice-nucleation chambers requires much higher INP concentrations, which is what we ultimately mean by higher detection limits.

To clarify, we have revised the text to "*However, ice nucleation chambers and reactors are typically expensive and have higher detection limits compared to DFTs. This enables them to measure often only at lower temperatures (T < –20 °C), particularly for typical atmospheric INP concentrations. Background noise caused by ice residues falling from chamber walls (e.g., CFDCs) or counting statistics of low ice crystal numbers make detecting INPs with low concentrations challenging (e.g., for both CFDCs and expansion chambers).*"

Lines 65–69: The references cited here are mostly about measurement campaigns and do not give detailed instrument descriptions. Moreover, they are all given as one list. Instead, they should be split up into microliter and picoliter setups, and into microfluidic devices and instruments working with well plates. References about measurement campaigns need to be replaced by references describing the instrument setup.

Thank you for your suggestion. In response to your previous comments, we have revised the cited references to include more classical and instrumental sources.

As for Lines 66–70, the revised text now reads: "*As an alternative, offline DFTs have been developed to measure the temperature-dependent freezing abilities of droplets containing aerosol particles. While different DFTs follow similar principles, the methods may differ for sample collection, droplet preparation, and sample cooling (Hill et al., 2014; Budke and Koop, 2015; Chen et al., 2018a; Miller et al., 2021; Chen et al., 2018b; Harrison et al., 2018; David et al., 2019; Steinke et al., 2020).*"

When comparing the DFTs' performance of MilliQ water samples, we include the droplet size information (Fig. 8 in the revised manuscript). Moreover, when summarizing the DFT instruments, we also include the droplet size information. However, we chose not to separate the microliter and picoliter setups, as we did not specifically discuss their common features or differences. We believe that dividing them would disrupt the logical flow of this section.

Lines 71–74: "Typically, the sampling time, droplet volume, and aerosol suspension concentration can be adjusted, which affects the particle number within each droplet and, thereby, its freezing ability. For example, particle numbers within a droplet can be enhanced by extending the aerosol sampling time, enlarging the droplet size, or reducing the dilution ratio of aerosol suspensions with water.": The possibilities of adjustment that are pointed out here are typically small, because most instruments can work only in a narrow volume range (within less than an order of magnitude). Variations in sampling time are also within a quite narrow range. Droplet experiments are usually performed with a cooling rate of 1 K/min because at higher cooling rates the temperature accuracy decreases and experiments at lower cooling rates become time consuming. The authors need to demonstrate the volume and cooling rate range that they can cover with their setup.

Thanks for your suggestions. In this study, we used a fixed cooling rate of 1 K min^{-1} and a droplet volume of 50 µL.

FINDA-WLU, similar to other DFTs, can change the droplet volume (a relatively narrow range) and the cooling rate range. However, the volume and cooling rate range may impact the temperature uncertainty, which means a companion calibration should be provided. We would perform such a calibration if experiments with different droplet sizes and cooling rates are needed.

We agree that the possibilities of adjusting droplet size for FINDA are small. But the aerosol sampling time and aerosol suspensions can be adjusted for a large range, e.g., we adjust the solution by about 2 and 9 orders of magnitude for ATD and Snomax® solutions. Also, if microfluidic chips are used for droplet generation, the volume can be largely modulated.

Lines 75–77: "In this way, this approach enables the quantification of low-concentration INP species in the atmosphere, which overcomes the high detection limitations of ice nucleation chambers. Due to these advantages, DFTs are widely used in current ice nucleation studies." DFTs operating with well plates are widely used because they are rather cheap and easy to use. Instruments working with smaller volumes like microfluidic devices and continuous flow diffusion chambers are complementary to well plate setups because they can monitor ice nucleation down to the homogeneous freezing threshold while setups with well plates only deliver results down to temperatures where freezing on "pure water" impurities sets in, which is well above the homogeneous freezing threshold. The limitations of the FINDA setup should be pointed out clearly. The temperature ranges covered with the different setups should be discussed.

We agree with you that (1) DFTs operating with well plates are widely used because they are rather cheap and easy to use; (2) Instruments working with smaller volumes, like microfluidic devices and continuous flow diffusion chambers, are complementary to well plate setups because they can monitor ice nucleation down to the homogeneous freezing threshold.

In lines 57-61, we include the above discussion:" *To measure the immersion freezing of droplets containing INPs, ice nucleation chambers are operated under mixed-phase cloud-relevant conditions, with T above –38 °C and RH with respect to water at ~100%. The continuous flow diffusion chambers (CFDCs) (Demott et al., 2017; Lacher et al., 2017; Demott et al., 2018; Brunner and Kanji, 2021) and cloud expansion chambers (Möhler et al., 2021a; Möhler et al., 2021b) are two types of ice nucleation chambers operating on different working principles."*

We also modified the text in Lines 61 to 65.

"However, ice nucleation chambers and reactors are typically expensive and have higher detection limits compared to DFTs. This enables them to measure often only at lower temperatures (T < –20 °C), particularly for typical atmospheric INP concentrations. Background noise caused by ice residues falling from chamber walls (e.g., CFDCs) or counting statistics of low ice crystal numbers make detecting INPs with low concentrations challenging (e.g., for both CFDCs and expansion chambers)."

Lines 101–102: "FINDA-WLU detects LED light reflected by freezing of water droplets placed in a 96-well PCR plate over time." Sentence needs to be improved.

The full sentence is "*Using a CCD camera (Fig. 1a), FINDA-WLU detects LED light reflected by freezing of water droplets placed in a 96-well PCR plate over time.*"

It was changed to: "*A CCD camera (Fig. 1a) is used to detect the reflected LED light over the water droplets placed in a 96-well PCR plate during the experiment.*"

Lines 103–104: "The camera is fixed above the PCR wells region using an adjustable camera zoom lens (12-120 mm Focal Length, Qiyun Photoelectric Co., China)." Sentence structure needs to be improved.

It was changed to: "*The camera is fixed above the region of the PCR wells using an adjustable zoom lens (12-120 mm Focal Length, Qiyun Photoelectric Co., China).*"

Lines 114–116: "These sensors are embedded and sealed within thermally conductive epoxy (Omegabond 200, Omega Engineering, Inc., USA) within tubes cut from a PCR plate, ensuring consistent heat transfer between the PCR plate and Pt100 sensors." How are the tubes cut? Does this mean that the commercial plates are modified?

We cut a well from the PCR and put the temperature sensor in the well, with thermally conductive

epoxy. Below is the figure of this setup.

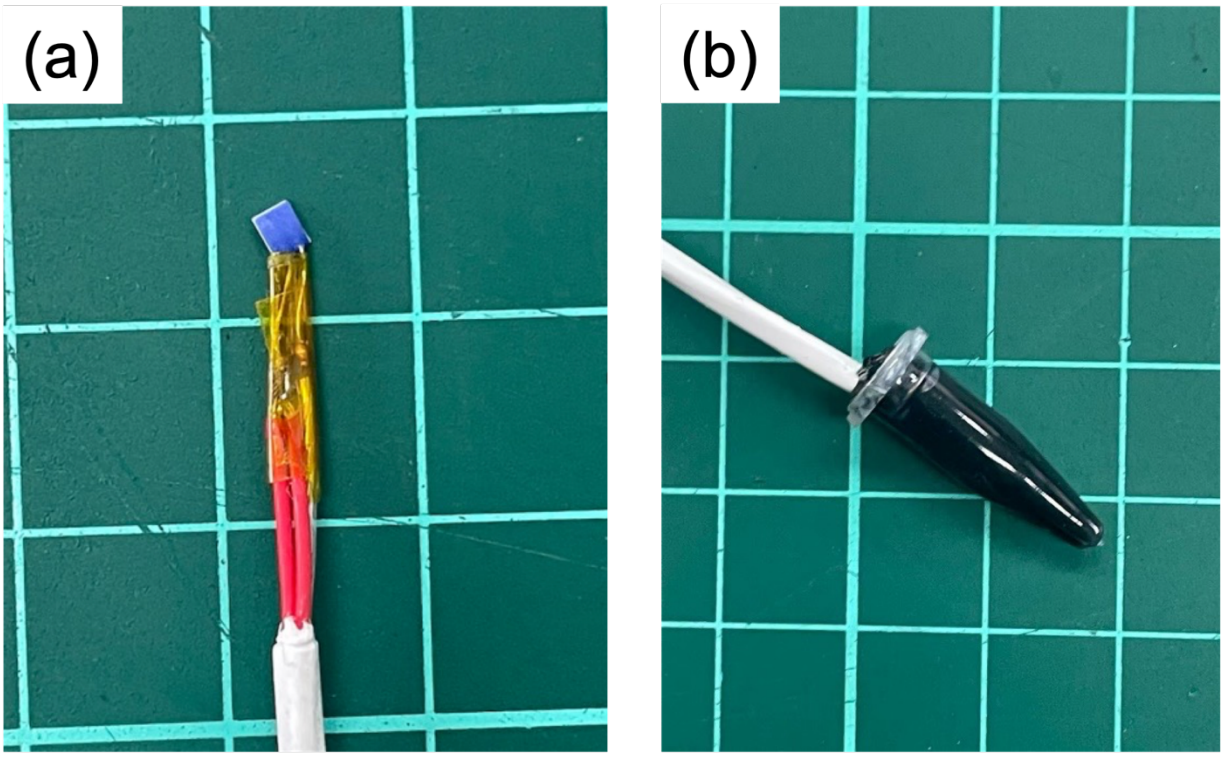

Fig C2. (a) The modified Pt100 sensors. (b) The modified Pt100 sensors with thermally conductive epoxy inside a PCR well.

The cut well is outside of the PCR plate, as shown in Fig. 1b and c. Therefore, the commercial plates are not modified in each experiment.

Lines 153–155: Figure 3 shows an increase in grayscale not a decrease. Please revise the text accordingly. Moreover, Fig. 3 shows that a large change in grayscale (by about 80) is always preceded by a smaller change by around 20 at about 1 K higher temperature. What makes you sure that the second larger change marks ice nucleation and not the smaller one at higher temperature? As the accuracy of the instrument is given as ± 0.6 K, it is important whether the first small or the second larger step marks nucleation. This needs to be investigated and discussed.

Figure 3 demonstrates a decrease in grayscale as the chamber cools. The figure should be interpreted from right to left, as the experiment represents a cooling process. Consequently, the first significant change in grayscale indicates the onset of ice nucleation. The second change in grayscale is caused by the freezing of the remaining droplet solution (David et al., 2019). We have also checked previously published papers, and most figures depict the temperature decrease from right to left. Therefore, we have decided to retain the figure as it is.

We modified the text accordingly: "*The grayscale value of a well stays constant until a sudden decrease is observed during a cooling experiment, indicating the onset of freezing. From 0.0 °C to −35.0 °C, the maximum decrease in grayscale value was used to identify the freezing event and the temperature at which it occurs.*"

Moreover, according to the infrared camera measured temperature during a cooling experiment (Fig. C1), only one latent heat release process happened. Similar to Fig. 5d in the manuscript, here we show the temperature profile of a well during the cooling process.

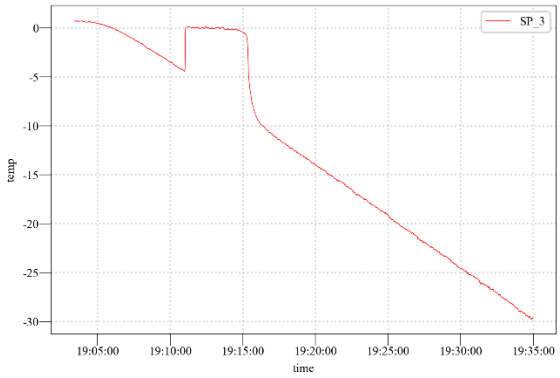

Fig. C1. The temperature profile of a well is measured by the infrared camera after its calibration.

Lines 235–236: "This phenomenon also explains why freezing is most often triggered at the droplet bottom from our observation." What observation do you refer to? Can you observe where freezing starts? Also, the temperature difference of just 1°C between the bottom and the top of the well is not sufficient to trigger freezing always from the bottom, especially when freezing occurs over a large temperature range.

In our experiment, we observed that ice nucleation began at the bottom of the PCR well, not only for FINDA-WLU but also for other PCR well-based cold stages. However, this observation cannot be demonstrated through the figures. Therefore, we have removed the sentence to avoid any ambiguity.

Lines 119–120, line 245, Figure 6: The figure shows that almost 5°C are required until the temperature difference becomes linear. As samples may freeze already at around -5°C, consider to starting the ramp at 5°C so that a good linearity is achieved when temperature reaches subzero temperatures. Just one cooling ramp is shown in Fig. 6. Have the cooling ramps been repeated? What is the reproducibility?

This experiment was repeated multiple times with multiple well positions in a PCR, and it is reproducible. We agree with you that starting the freezing from 5 °C will solve this problem.

Importantly, the purpose of this test in Fig. 6 is to verify which temperatures (bottom of the aluminum block, bottom of the empty PCR plate, Milli-Q water surface, and ethanol surface) should be used for horizontal temperature calibration. Section 2.4.3 and Figure 6 do not include the temperature calibration; therefore, the non-linear correlation above –5 °C will not affect the calibration results.

Line 250: David et al. (2019) does not use an aluminium block.

In the original text, we stated:" *The temperature bias across 96-well PCR plates has been discussed for aluminum block-based instruments with simulations (Beall et al., 2017), calibration substance freezing experiments (Kunert et al., 2018), and by comparison of temperature differences between corner and center wells (David et al., 2019).*"

We are trying to say that David et al. (2019) compares the temperature differences between the corner and center wells. We did not mean it use the aluminum block-based instruments, but Beall et al. (2017) use the aluminum block-based instrument.

Line 265, Figure 7: how many times has the well calibration experiment been performed? What was the variability between experiments? Has it been performed with different PCR plates? There might be additional variability introduced when the position of the plates within the block has some variability.

We performed the single-well calibration experiment only once. As we responded in the previous comments, the horizontal temperature heterogeneity is caused by the ethanol circulation in the chiller, which has been discussed in previous studies, e.g., the DRoplet Ice Nuclei Counter Zurich (DRINCZ) (David et al., 2019), IR-NIPI (Harrison et al., 2018), and Micro-PINGUIN (Wieber et al., 2024). For a specific chiller and fixed temperature cooling rate, we assume the temperature deviation is reproducible.

The horizontal temperature distribution might slightly change over time. To avoid the bias of temperature calibration, we do the whole temperature calibration procedure yearly.

We used PCR plates from the same brand, as different brands may have varying thermal conductivities. Therefore, when using PCR plates from different brands, additional temperature calibration is required.

The aluminum block is fixed inside the chiller, ensuring that the PCR position remains consistent across all experiments.

Line 333: The method by Agresti and Coull (1998) should be described in some sentences.

It was explained in Lines 281-284.

"$C_{INP}(T)$ *is calculated from statistical analysis; therefore, it is necessary to assess the reliability of the results. According to the binomial distribution method proposed by Agresti and Coull (1998), the 95% confidence interval of the* FF *at temperature* T, $CI_{95\%}(T)$, *is calculated as…*"

Line 346, Figure 9: Can you specify what kind of uncertainty the shaded area shows? Min-max or percentiles? How many times was a measurement repeated?

The corresponding shaded areas indicate the 95% confidence interval of n_{m}, derived by Agresti and Coull (1998). We modified the figure caption accordingly.

Line 355: a reference to Fig. A2 in the appendix would be helpful here.

As all FF of Snomax are from this study, a reference to Fig. A2 is not needed.

Line 369: References to the “previous studies” should be given.

Done. We added previous studies (Wieber et al., 2024; Tarn et al., 2018; Polen et al., 2016).

Line 373, Figure 10: the figure caption needs to be reformulated. Moreover, the references to the studies should be added. The freezing experiments seem to have been carried out several times as uncertainty ranges are indicated in the figures. It needs to be stated how many times.

The references are added.

We only did one experiment for each dilution of the Snomax® samples. The uncertainty range is the 95% confidence interval of n_{m}, derived by Agresti and Coull (1998).

Technical comments:

Line 220: “bottom of the” instead of “bottom of”

Changed.

Line 332: “Fig. 6” should be “Fig. 9”

Changed.

Line 335: “overlapping” instead of “overlapped”

Changed.

Line 351: “bacteria” instead of “bacteriuma”

Changed.

Line 356: “scale” instead of “are scaled”

Changed.

Line 370: “Caution” instead of “Cautions”

Changed.

Line 380: “overlapping” instead of “overlapped”

Changed.

Line 381: “who” instead of “which”

Changed.

Reference:

Miller, A. J., Brennan, K. P., Mignani, C., Wieder, J., David, R. O., and Borduas-Dedekind, N.: Development of the drop Freezing Ice Nuclei Counter (FINC), intercomparison of droplet freezing techniques, and use of soluble lignin as an atmospheric ice nucleation standard, Atmos. Meas. Tech., 14, 3131–3151, https://doi.org/10.5194/amt-14-3131-2021, 2021.

Reference:

Agresti, A. and Coull, B. A.: Approximate is Better than "Exact" for Interval Estimation of Binomial Proportions, The American Statistician, 52, 119-126, 10.1080/00031305.1998.10480550, 1998.

Beall, C. M., Stokes, M. D., Hill, T. C., DeMott, P. J., DeWald, J. T., and Prather, K. A.: Automation and heat transfer characterization of immersion mode spectroscopy for analysis of ice nucleating particles, Atmospheric Measurement Techniques, 10, 2613-2626, 10.5194/amt-10-2613-2017, 2017.

Brunner, C. and Kanji, Z. A.: Continuous online monitoring of ice-nucleating particles: development of the automated Horizontal Ice Nucleation Chamber (HINC-Auto), Atmospheric Measurement Techniques, 14, 269-293, 10.5194/amt-14-269-2021, 2021.

Budke, C. and Koop, T.: BINARY: an optical freezing array for assessing temperature and time dependence of heterogeneous ice nucleation, Atmospheric Measurement Techniques, 8, 689-703, 10.5194/amt-8-689-2015, 2015.

Chen, J., Pei, X., Wang, H., Chen, J., Zhu, Y., Tang, M., and Wu, Z.: Development, Characterization, and Validation of a Cold Stage-Based Ice Nucleation Array (PKU-INA), Atmosphere, 9, 357, https://doi.org/10.3390/atmos9090357, 2018a.

Chen, J., Wu, Z., Augustin-Bauditz, S., Grawe, S., Hartmann, M., Pei, X., Liu, Z., Ji, D., and Wex, H.: Ice-nucleating particle concentrations unaffected by urban air pollution in Beijing, China, Atmospheric Chemistry and Physics, 18, 3523-3539, 10.5194/acp-18-3523-2018, 2018b.

David, R. O., Cascajo-Castresana, M., Brennan, K. P., Rösch, M., Els, N., Werz, J., Weichlinger, V., Boynton, L. S., Bogler, S., Borduas-Dedekind, N., Marcolli, C., and Kanji, Z. A.: Development of the DRoplet Ice Nuclei Counter Zurich (DRINCZ): validation and application to field-collected snow samples, Atmos. Meas. Tech., 12, 6865-6888, 10.5194/amt-12-6865-2019, 2019.

DeMott, P. J., Prenni, A. J., McMeeking, G. R., Sullivan, R. C., Petters, M. D., Tobo, Y., Niemand, M., Möhler, O., Snider, J. R., Wang, Z., and Kreidenweis, S. M.: Integrating laboratory and field data to quantify the immersion freezing ice nucleation activity of mineral dust particles, Atmos. Chem. Phys., 15, 393-409, 10.5194/acp-15-393-2015, 2015.

DeMott, P. J., Hill, T. C. J., Petters, M. D., Bertram, A. K., Tobo, Y., Mason, R. H., Suski, K. J., McCluskey, C. S., Levin, E. J. T., Schill, G. P., Boose, Y., Rauker, A. M., Miller, A. J., Zaragoza, J., Rocci, K., Rothfuss, N. E., Taylor, H. P., Hader, J. D., Chou, C., Huffman, J. A., Pöschl, U., Prenni, A. J., and Kreidenweis, S. M.: Comparative measurements of ambient atmospheric concentrations of ice nucleating particles using multiple immersion freezing methods and a

continuous flow diffusion chamber, Atmospheric Chemistry and Physics, 17, 11227-11245, 10.5194/acp-17-11227-2017, 2017.
DeMott, P. J., Möhler, O., Cziczo, D. J., Hiranuma, N., Petters, M. D., Petters, S. S., Belosi, F., Bingemer, H. G., Brooks, S. D., Budke, C., Burkert-Kohn, M., Collier, K. N., Danielczok, A., Eppers, O., Felgitsch, L., Garimella, S., Grothe, H., Herenz, P., Hill, T. C. J., Höhler, K., Kanji, Z. A., Kiselev, A., Koop, T., Kristensen, T. B., Krüger, K., Kulkarni, G., Levin, E. J. T., Murray, B. J., Nicosia, A., O'Sullivan, D., Peckhaus, A., Polen, M. J., Price, H. C., Reicher, N., Rothenberg, D. A., Rudich, Y., Santachiara, G., Schiebel, T., Schrod, J., Seifried, T. M., Stratmann, F., Sullivan, R. C., Suski, K. J., Szakáll, M., Taylor, H. P., Ullrich, R., Vergara-Temprado, J., Wagner, R., Whale, T. F., Weber, D., Welti, A., Wilson, T. W., Wolf, M. J., and Zenker, J.: The Fifth International Workshop on Ice Nucleation phase 2 (FIN-02): laboratory intercomparison of ice nucleation measurements, Atmospheric Measurement Techniques, 11, 6231-6257, 10.5194/amt-11-6231-2018, 2018.
Garimella, S., Kristensen, T. B., Ignatius, K., Welti, A., Voigtländer, J., Kulkarni, G. R., Sagan, F., Kok, G. L., Dorsey, J., Nichman, L., Rothenberg, D. A., Rösch, M., Kirchgäßner, A. C. R., Ladkin, R., Wex, H., Wilson, T. W., Ladino, L. A., Abbatt, J. P. D., Stetzer, O., Lohmann, U., Stratmann, F., and Cziczo, D. J.: The SPectrometer for Ice Nuclei (SPIN): an instrument to investigate ice nucleation, Atmos. Meas. Tech., 9, 2781-2795, 10.5194/amt-9-2781-2016, 2016.
Harrison, A. D., Whale, T. F., Rutledge, R., Lamb, S., Tarn, M. D., Porter, G. C. E., Adams, M. P., McQuaid, J. B., Morris, G. J., and Murray, B. J.: An instrument for quantifying heterogeneous ice nucleation in multiwell plates using infrared emissions to detect freezing, Atmospheric Measurement Techniques, 11, 5629-5641, 10.5194/amt-11-5629-2018, 2018.
Hill, T. C. J., Moffett, B. F., DeMott, P. J., Georgakopoulos, D. G., Stump, W. L., and Franc, G. D.: Measurement of Ice Nucleation-Active Bacteria on Plants and in Precipitation by Quantitative PCR, Applied and Environmental Microbiology, 80, 1256, 10.1128/AEM.02967-13, 2014.
Kanji, Z. A., Welti, A., Chou, C., Stetzer, O., and Lohmann, U.: Laboratory studies of immersion and deposition mode ice nucleation of ozone aged mineral dust particles, Atmos. Chem. Phys., 13, 9097-9118, 10.5194/acp-13-9097-2013, 2013.
Kunert, A. T., Lamneck, M., Helleis, F., Pöschl, U., Pöhlker, M. L., and Fröhlich-Nowoisky, J.: Twin-plate Ice Nucleation Assay (TINA) with infrared detection for high-throughput droplet freezing experiments with biological ice nuclei in laboratory and field samples, Atmospheric Measurement Techniques, 11, 6327-6337, 10.5194/amt-11-6327-2018, 2018.
Lacher, L., Lohmann, U., Boose, Y., Zipori, A., Herrmann, E., Bukowiecki, N., Steinbacher, M., and Kanji, Z. A.: The Horizontal Ice Nucleation Chamber (HINC): INP measurements at conditions relevant for mixed-phase clouds at the High Altitude Research Station Jungfraujoch, Atmospheric Chemistry and Physics, 17, 15199-15224, 10.5194/acp-17-15199-2017, 2017.
Miller, A. J., Brennan, K. P., Mignani, C., Wieder, J., David, R. O., and Borduas-Dedekind, N.: Development of the drop Freezing Ice Nuclei Counter (FINC), intercomparison of droplet freezing techniques, and use of soluble lignin as an atmospheric ice nucleation standard, Atmos. Meas. Tech., 14, 3131-3151, 10.5194/amt-14-3131-2021, 2021.
Möhler, O., Adams, M., Lacher, L., Vogel, F., Nadolny, J., Ullrich, R., Boffo, C., Pfeuffer, T., Hobl, A., Weiß, M., Vepuri, H. S. K., Hiranuma, N., and Murray, B. J.: The Portable Ice Nucleation Experiment (PINE): a new online instrument for laboratory studies and automated long-term field observations of ice-nucleating particles, Atmospheric Measurement Techniques, 14, 1143-1166, 10.5194/amt-14-1143-2021, 2021a.

Möhler, O., Adams, M., Lacher, L., Vogel, F., Nadolny, J., Ullrich, R., Boffo, C., Pfeuffer, T., Hobl, A., Weiß, M., Vepuri, H. S. K., Hiranuma, N., and Murray, B. J.: The Portable Ice Nucleation Experiment (PINE): a new online instrument for laboratory studies and automated long-term field observations of ice-nucleating particles, Atmos. Meas. Tech., 14, 1143-1166, 10.5194/amt-14-1143-2021, 2021b.
Polen, M., Lawlis, E., and Sullivan, R. C.: The unstable ice nucleation properties of Snomax® bacterial particles, Journal of Geophysical Research: Atmospheres, 121, 11,666-611,678, 10.1002/2016JD025251, 2016.
Ren, Y., Fu, S., Bi, K., Zhang, H., Lin, X., Cao, K., Zhang, Q., and Xue, H.: Freezing Nucleus Spectra for Hailstone Samples in China From Droplet Freezing Experiments, Journal of Geophysical Research: Atmospheres, 129, e2023JD040505, 10.1029/2023JD040505, 2024.
Rogers, D. C.: Development of a continuous flow thermal gradient diffusion chamber for ice nucleation studies, Atmospheric Research, 22, 149-181, https://doi.org/10.1016/0169-8095(88)90005-1, 1988.
Rogers, D. C., DeMott, P. J., Kreidenweis, S. M., and Chen, Y.: A Continuous-Flow Diffusion Chamber for Airborne Measurements of Ice Nuclei, J. Atmos. Oceanic Technol., 18, 725-741, 10.1175/1520-0426(2001)018<0725:ACFDCF>2.0.CO;2, 2001.
Steinke, I., Hiranuma, N., Funk, R., Höhler, K., Tüllmann, N., Umo, N. S., Weidler, P. G., Möhler, O., and Leisner, T.: Complex plant-derived organic aerosol as ice-nucleating particles – more than the sums of their parts?, Atmospheric Chemistry and Physics, 20, 11387-11397, 10.5194/acp-20-11387-2020, 2020.
Tarn, M. D., Sikora, S. N. F., Porter, G. C. E., O'Sullivan, D., Adams, M., Whale, T. F., Harrison, A. D., Vergara-Temprado, J., Wilson, T. W., Shim, J.-u., and Murray, B. J.: The study of atmospheric ice-nucleating particles via microfluidically generated droplets, Microfluidics and Nanofluidics, 22, 52, 10.1007/s10404-018-2069-x, 2018.
Wieber, C., Rosenhøj Jeppesen, M., Finster, K., Melvad, C., and Šantl-Temkiv, T.: Micro-PINGUIN: microtiter-plate-based instrument for ice nucleation detection in gallium with an infrared camera, Atmos. Meas. Tech., 17, 2707-2719, 10.5194/amt-17-2707-2024, 2024.